*Progress In Electromagnetics Research C, Vol. 40, 229–242, 2013*

# WIDE BEAMWIDTH QUADIFILAR HELIX ANTENNA WITH CROSS DIPOLES

**Wei Xin Lin and Qing Xin Chu**[*]

School of Electronic and Information Engineering, South China University of Technology, Guangzhou 510640, China

**Abstract**—A simple and novel method for increasing the gain at low elevation angle and widening the beamwidth of quadrifilar helix antenna (QHA) is presented. By adding cross dipoles as a reflector, the right hand circular polarization (RHCP) gain at 5° elevation angle ($\theta = 85^\circ$) increases by about 1.4 dB. Parametric studies are performed to explore the performance improvements. An antenna for CNSS (Compass Navigation Satellite System, 2.492 GHz) application is realized based on the studies. The RHCP gain at 5° elevation angle is about 0.6 dB, and 3 dB beamwidth is greater than 220°. 10 dB impedance bandwidth is more than 24%, and 3 dB axial ratio bandwidth is more than 32%. Measured results are presented to validate the proposed method.

## 1. INTRODUCTION

In recent years, satellite communication systems have been widely applied, such as broadcasting satellite communication system and GPS (global positioning system) [1]. CP antennas are very suitable for these applications because of flexibility in orientation angle between transmitter and receiver antennas. For global positioning systems, uniform pattern coverage over the entire upper hemisphere is required. It is known that signal at low elevation angle has a great contribution to precision of the positioning based on the positioning principle, but the satellites in this direction are farther from the ground than the satellites in the zenith direction. In order to enhance the positioning precision, antennas with high gain at low elevation angle are needed, and especially for the CNSS, strict requirement for the gain at low

---

*Received 24 April 2013, Accepted 26 May 2013, Scheduled 3 June 2013*

[*] Corresponding author: Qing Xin Chu (qxchu@scut.edu.cn).

elevation angle is set. Sometimes CP gain more than $-0.5$ dB at 5° elevation angle is required. However, for most CP antennas the gain at low elevation angle is generally low. In addition, CP antennas with 3 dB beamwidth greater than 220° is required for some applications such as ship because of severe shaking. But most CP antennas do not have such wide beamwidth.

Quadrifilar helix antenna [2–4] has many advantages, such as cardioid shaped pattern with excellent CP coverage, good axial ratio, simple structure, light weight and low cost, which make it a very attractive candidate for global positioning system application. The conventional quadrifilar helix antenna is composed of four helical elements. The four helical elements are fed in with the same amplitude and sequential phase difference (PD) of 90°. QHA can be seen as consisting of two pairs of bifilar helix antennas which are placed orthogonally in space and fed in with the same amplitude and quadrature phase.

Although compared to conventional planar CP microstrip antenna whose 3 dB beamwidth is generally about 60°–100° [5–9], QHA has wide beamwidth characteristic, in order to satisfy the enhancement of the positioning precision, especially the requirement of the gain at low elevation angle of CNSS, the gain at low elevation angle of conventional QHA needs further improvement. Besides, in order to realize wide beamwidth characteristic by conventional QHA, the geometric parameters should be optimized repeatedly and the optimization process is very cumbersome and time-consuming.

At present, the study for increasing the gain at low elevation angle of CP antenna and widening the beamwidth is very rare. Some techniques for realizing wide beamwidth using QHA [10–13] and planar CP antenna [14–19] have been put forward. The simplest method to widen the beamwidth of QHA is changing the size and shape of the ground plane [10], but the effect is very limited. Four-arm conical spiral antenna [11] can realize wide beamwidth, but the effect on increasing the gain at low elevation angle is also limited and has the disadvantages of large size and complex structure. Placing a parasitic loop of right size above QHA [12] could change radiation pattern and increase the gain at low elevation angle. The effect of a pair of half-wave dipoles and quarter-wave monopoles on the radiation pattern of the cone type helix antenna has been studied in [13].

In this paper, a simple method to increase the CP gain at low elevation angle and widen the beamwidth of the QHA is presented. Compared to the study in [13], the length of the cross dipoles is no longer fixed in half wavelength and the relationship between the length of the parasitic cross dipoles and the radiation pattern of the

CP antenna is studied and explained. Further, detailed quantified values are given in our work. By placing a cross dipoles unit above QHA and adjusting the length of the dipoles and the vertical distance between the dipoles and the top of QHA, the radiation pattern could be easily changed to have a wider beamwidth and the gain at low elevation angle would increase accordingly. The radiation pattern, return loss and axial ratio results of the proposed antenna compared with the conventional QHA are presented in this paper. The effect of the parameters of the cross dipoles unit is studied. Finally, an antenna for CNSS application is realized based on the studies. The RHCP gain at 5° elevation angle is about 0.6 dB and the impedance bandwidth is more than 24%. The measure result is presented to validate the proposed method.

## 2. ANTENNA STRUCTURE

### 2.1. Configuration of the QHA with Cross Dipoles

The configuration of the proposed antenna is shown in Figure 1(a). The antenna consists of four helix-shaped radiating elements, mounted on a circular ground plane. Each element is about half wavelength long and all the elements are shorted by a ring at the top of the helix. The

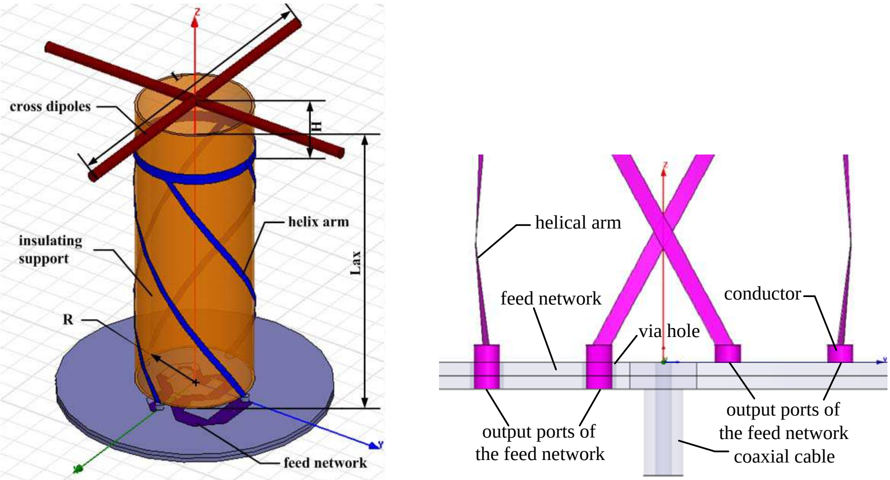

(a) (b)

**Figure 1.** The geometry of (a) the QHA with cross dipoles and (b) the detail of antenna feed.

parameters of the QHA can be set by:

$$L_{ax} = \sqrt{(L_{ele} - R)^2 - (2\pi R \cdot L_{ax}/P)^2} \tag{1}$$

where $L_{ele}$ is the length of each helix element, $R$ the radius of the QHA, $L_{ax}$ the axial length of the QHA, and $P$ the pitch of the helix arm.

The four helical elements are fed with same amplitude and quadrature phases. The detail of the antenna feed is shown in Figure 1(b). Four helical arms are connected with the output ports of the feed network, which is fed with coaxial cable. Because the feed network has two layers, two helical arms should connect the output ports at the bottom layer through via holes. As a parasitic element, a cross dipoles unit is placed above the QHA. This element can be supported by some insulating material. Geometry parameters of the proposed antenna and referenced conventional QHA are shown in Table 1. $L$ is defined as the length of each dipole and $H$ defined as the vertical distance between the dipoles and the top of the QHA.

**Table 1.** Geometry parameters and RHCP gain at $\theta = 85°$ and $\theta = 0°$ of the proposed antenna and the referenced conventional QHA without cross dipoles.

| | Without cross dipole | Cross dipole as director | Cross dipole as reflector |
|---|---|---|---|
| $R$ (mm) | 11 | 11 | 11 |
| $L_{ax}$ (mm) | 52 | 52 | 52 |
| $P$ (mm) | 138 | 138 | 138 |
| $L$ (mm) | - | 50 | 70 |
| $H$ (mm) | - | 15 | 15 |
| $\theta = 85°$ RHCP gain (dB) | 0.14 | -2.40 | 1.14 |
| $\theta = 0°$ RHCP gain (dB) | 3.18 | 5.65 | 0.14 |

Figure 2 shows the vector current distribution of QHA and crossed dipole in 0° and 90°. The radiation field of the QHA excites induced current in the cross dipoles, and the induced current also radiates CP wave. Because of the existence of the cross dipoles, the distribution of the radiation field is changed. Figure 3 presents the simulated result of radiation patterns in 3 different cases (without cross dipoles, dipole length less than and more than half wavelength). When the length of the dipoles is slightly less than half wavelength (here set the length of the dipole as $0.417\lambda$), the cross dipoles unit can be seen as a director,

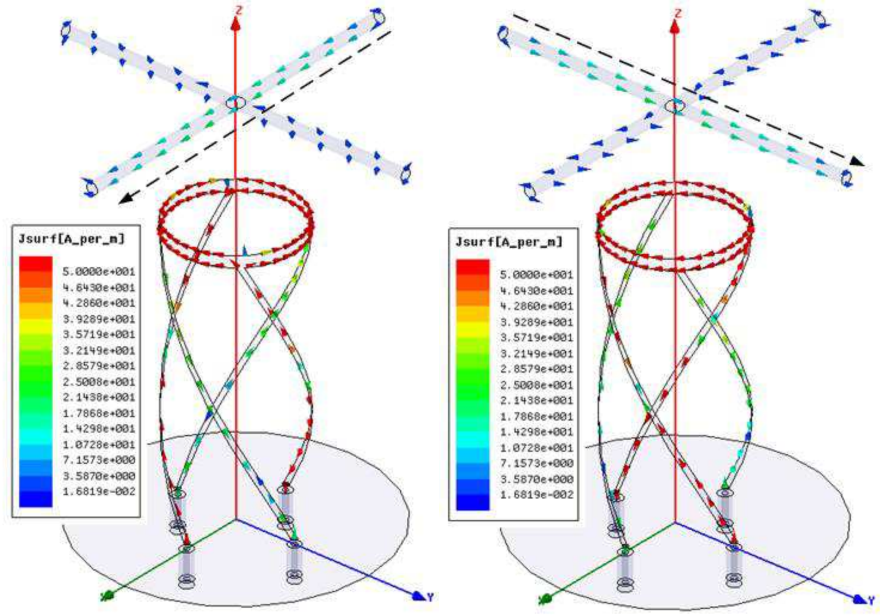

(a) (b)

**Figure 2.** The vector current distribution of the proposed antenna at 2.5 GHz in (a) $t = 0°$ and (b) $t = 90°$.

which strengthens the radiation at axial direction and weakens the radiation at low elevation angle and as a result makes the beamwidth narrower. When the length of the dipoles is slightly greater than half wavelength (here set the length of the dipole as $0.58\lambda$), the cross dipoles unit can be seen as a reflector, which suppresses the radiation at axial direction and strengthens the radiation at low elevation angle and as a result makes the beamwidth wider. This is somewhat similar to the principle of Yagi-Uda antenna. However, it is more complex than Yagi-Uda antenna because of the distributed tridimensional structure of QHA. Adjusting the dipole length and the vertical distance between the dipole and the top of QHA with other geometry parameters unchanged, the radiation pattern and the gain can be easily changed. In Figure 3, we can note that by adding cross dipoles as a reflector, the RHCP gain at 5° elevation angle is increased to about 1 dB and the 3 dB beamwidth greater than 190°. How gain varies with the distance between crossed dipole and QHA changes will be discussed in parametric study section.

Figure 4 presents the simulation result of the return loss in 3 different cases (without cross dipoles, dipole length less than and more than half wavelength). From the result we observe that the

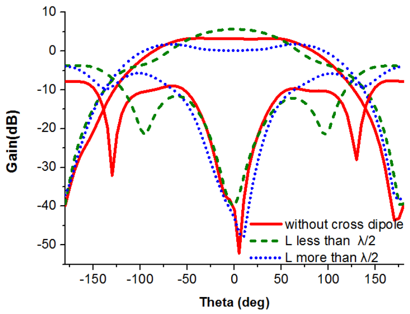

**Figure 3.** Comparison of radiation patterns in 3 different cases (without cross dipoles, dipole length less than and more than half wavelength).

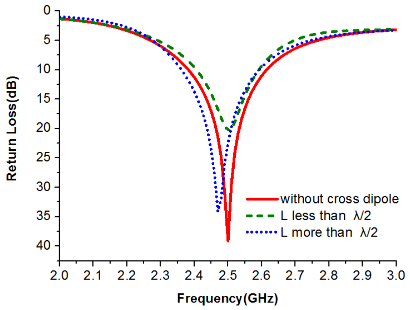

**Figure 4.** Comparison of return loss in 3 different cases (without cross dipoles, dipole length less than and more than half wavelength).

resonant frequency of the QHA with cross dipoles is slightly shifted compared to the case of the QHA without cross dipoles. This is because the mutual coupling between the cross dipoles and the QHA. The intrinsic resonant frequency of the parasitic cross dipole unit which works as a reflector is lower than that of the QHA, and therefore the resonant frequency of the whole antenna is lower than that of the QHA. When the parasitic unit works as a director, its intrinsic resonant frequency is higher than that of the QHA, and therefore the resonant frequency of the whole antenna is higher than that of the QHA. The 10 dB impedance bandwidth almost remains the same.

## 2.2. Realization of the Feed Network

A compact feed network proposed in our previous work [20] is used to feed the proposed antenna. Two Wilkinson power dividers are used as the feed network, providing sequential PD of 90° and same amplitude. Here Port 0 is defined as the input port and Ports 1, 2, 3 and 4 are defined as the output ports.

The detailed parameters of the feed network are shown in Figure 5. Two symmetric Wilkinson power dividers are assembled back to back with the common ground in the middle layer. The relative permittivity of the substrate $\varepsilon_r = 4.4$, the thickness $h = 0.8\,\text{mm}$ and the radius is 25 mm.

Figure 6 and Figure 7 present the simulated amplitude response, return loss and the PD of the output ports of the feed network, respectively. The results show that the power distribution in four output ports and the PD between any two adjacent output ports are

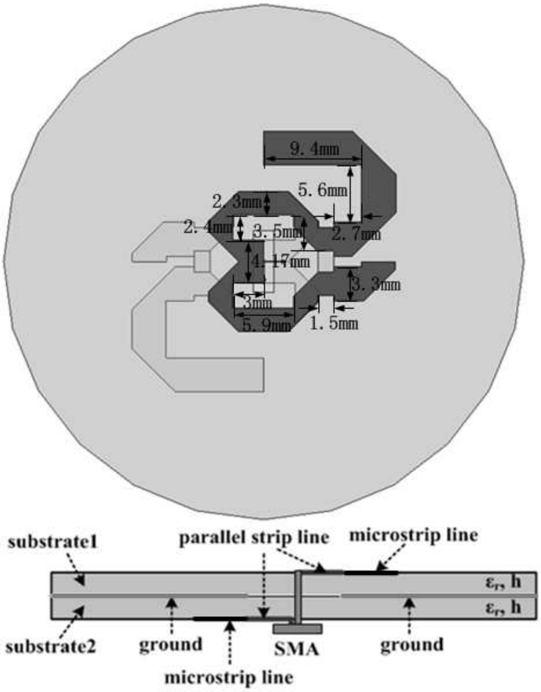

**Figure 5.** The realized feed network with power divider and phase shift.

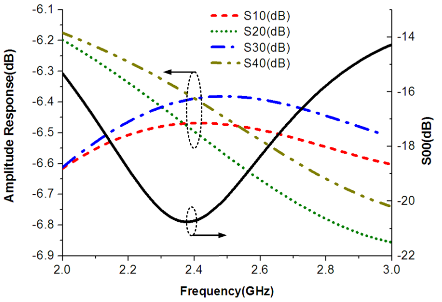

**Figure 6.** The simulated amplitude response and return loss of the feed network.

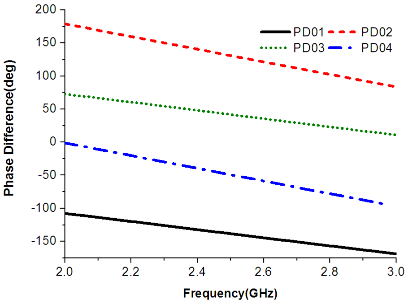

**Figure 7.** The simulated phase difference of the output ports of the feed network.

stable on broad frequency band. Over the frequency range of 2.2–2.8 GHz (24%), the amplitude responses, $S_{10}$, $S_{20}$, $S_{30}$ and $S_{40}$, are ranging from $-6.2$ to $-6.8$ dB and the PD between any two adjacent output ports are about $90^\circ \pm 10^\circ$ along with the $S_{00} < 15$ dB. By using this kind of feed network the QHA could have wideband characteristic.

## 3. PARAMETRIC STUDY

In this section, we study the effect of the geometry parameters of the dipole when it works as a reflector on the gain. The main parameters are the length of each dipole "$L$" and the vertical distance between the dipole and the top of QHA "$H$", as shown in Figure 1. The radius of each dipole is set as 1 mm and the geometry parameters of the QHA are set as the same with that shown in Table 1.

### 3.1. The Effect of the Length of Each Dipole

Several values of $L$ were used in simulations ($L$ = 64, 70, 76, 82 and 88 mm) while another parameter is fixed with value of $H = 15$ mm.

The radiation patterns for different values of $L$ are shown in Figure 8. We can observe that with the increase of the value of $L$, energy tends to concentrate to the axial direction. The direction where the maximum RHCP gain exists moves from $\theta = 75^\circ$ to $\theta = 60^\circ$ and the maximum RHCP gain gradually increases. The RHCP gain at $\theta = 0^\circ$ increases from $-0.82$ dB to 0.83 dB. The RHCP gain at 5° elevation angle ($\theta = 85^\circ$) slightly decreases, from 1.26 dB to 0.89 dB; however, it is obviously higher than that of the antenna without cross dipole. The return loss and the CP performance changes negligibly. Table 2

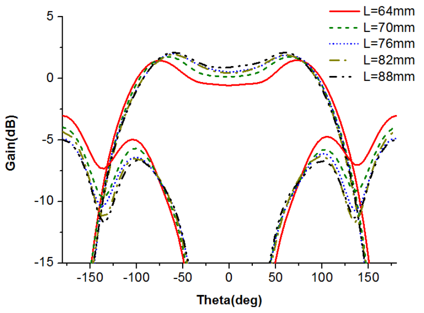

**Figure 8.** The radiation patterns for different values of $L$.

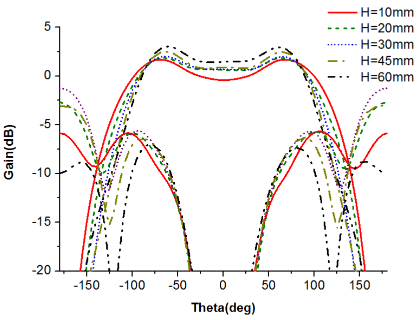

**Figure 9.** The radiation patterns for different values of $H$.

**Table 2.** The maximum RHCP gain and RHCP gain at $\theta = 85°$ and $\theta = 0°$ for different values of $L$.

| $L$ (mm) | 64 | 70 | 76 | 82 | 88 |
|---|---|---|---|---|---|
| $\theta = 85°$ RHCP gain (dB) | 1.26 | 1.14 | 0.90 | 0.89 | 0.89 |
| $\theta = 0°$ RHCP gain (dB) | −0.82 | 0.16 | 0.45 | 0.54 | 0.83 |
| Max RHCP gain (dB) | 1.51 | 1.73 | 1.91 | 1.96 | 2.08 |

gives the RHCP gain at the direction of $\theta = 0°$ and $\theta = 85°$, and the maximum RHCP gain for different values of $L$.

### 3.2. The Effect of the Vertical Distance between the Dipole and the Top of the QHA

Several values of $H$ were used in simulations ($H = 10$, 20, 30, 45 and 60 mm) while another parameter is fixed with value of $L = 70$ mm.

In Figure 9, we present the radiation patterns for different values of $H$. It is noted that with the increase of value $H$, the back lobe is suppressed with the RHCP gain at $\theta = 140°$, which decreases from −10 dB to −17 dB. The direction of the maximum RHCP gain remains at 25° elevation angle while the value gradually increases. The RHCP gain of the axial direction gets higher when the value of $H$ increases, changing from −0.41 dB to 1.49 dB. And the RHCP gain at 5° elevation angle almost maintains about 1 dB, obviously higher than that of the antenna without cross dipole. At the same time, the return loss and the CP performance basically remain the same. Table 3 gives the RHCP gain at $\theta = 0°$, $\theta = 65°$ and $\theta = 85°$ for different values of $H$.

**Table 3.** The RHCP gain at $\theta = 0°$, $\theta = 65°$ and $\theta = 85°$ for different values of $H$.

| $H$ (mm) | 10 | 20 | 30 | 45 | 60 |
|---|---|---|---|---|---|
| $\theta = 0°$ RHCP gain (dB) | −0.41 | 0.62 | 0.68 | 0.90 | 1.46 |
| $\theta = 65°$ RHCP gain (dB) | −0.03 | 0.71 | 0.76 | 0.80 | 1.48 |
| $\theta = 85°$ RHCP gain (dB) | 1.21 | 0.97 | 0.93 | 1.12 | 0.94 |

## 4. EXPERIMENTAL RESULTS

In order to validate the proposed design method, an antenna working at 2.492 GHz for CNSS application had been realized. Geometry parameters as optimized in Section 3 are adjusted. To realize the physical model, the characteristics of which are shown in Table 4.

**Table 4.** The physical characteristics of the realized antenna.

| | |
|---|---|
| $R$ (mm) | 11 |
| $L_{ax}$ (mm) | 49 |
| $P$ (mm) | 125 |
| $L$ (mm) | 64 |
| $H$ (mm) | 20 |

The final configuration of the antenna is shown in Figure 10. Four helical arms are manufactured with iron wires and coiled on the thin cylindrical cardboard. The cross dipoles are made with copper rods and supported by the cardboard. Since the antenna is handmade, there is fabrication error to maintain construction symmetry which is very important for the performance of the antenna. All simulations in this paper are done using commercial software Ansoft High Frequency Structure Simulator (HFSS12). Agilent N5230 network analyzer and microwave anechoic chamber are utilized for gain measurements of the antenna.

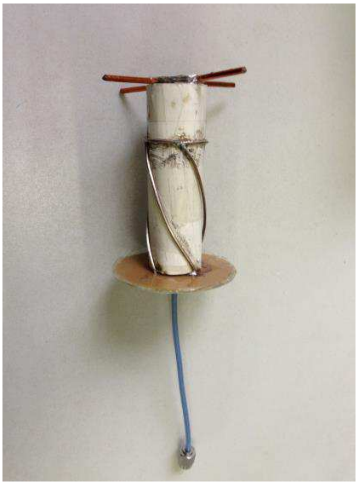

**Figure 10.** Photograph of the realized antenna.

In Figure 11, the measured and simulated return losses of the realized antenna are presented and compared with the simulated return loss of the QHA without cross dipoles. It is noted that the return loss performances of the antennas with and without cross dipoles are almost the same with 10 dB impedance bandwidth of more than 24% for the

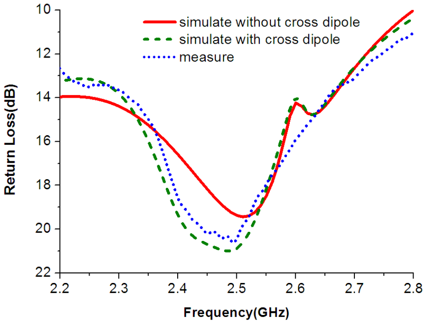

**Figure 11.** The measured and simulated return loss of the realized antenna along with the simulated result of the QHA without cross dipoles.

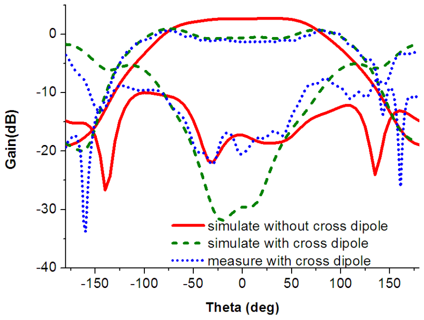

**Figure 12.** The simulated and measured CP gain patterns of the realized antenna along with the simulated result of the QHA without cross dipoles.

design frequency. The broadband antenna characteristic results from the feed network. The measured result is in good agreement with the simulated one.

Comparison of the simulated and measured CP gain patterns of the realized antenna along with the simulated result of the QHA without cross dipoles is shown in Figure 12. The measured result is in good agreement with the simulated one. Compared with the conventional QHA, the radiation energy of the antenna with cross dipoles shifts from the direction of high elevation angle to low elevation angle, and the 3 dB beamwidth is widened to greater than 220°. At the same time, the RHCP gain at 5° elevation angle increases from $-0.74$ dB to 0.65 dB. The RHCP gain of the axial direction decreases from 2.62 dB to $-0.6$ dB. And the direction of the maximum RHCP gain shifts from the axial direction to 15° elevation angle. Over the upper hemisphere, the RHCP gain is basically greater than $-0.6$ dB.

Figure 13 presents the simulated and measured results of the RHCP gain at 5° elevation angle versus frequency. We can note that the RHCP gain is maintained stable in a wide band and that the measured result is in a good agreement with the simulated one.

The simulated and measured axial ratios at broadside versus frequency are shown in Figure 14. The measured result is in good agreement with the simulated one. The antenna has broadband CP performance, and the 3 dB axial ratio bandwidth is more than 32%.

The comparison of the performances of the proposed antenna and the referenced conventional QHA without the cross dipoles is shown in Table 5.

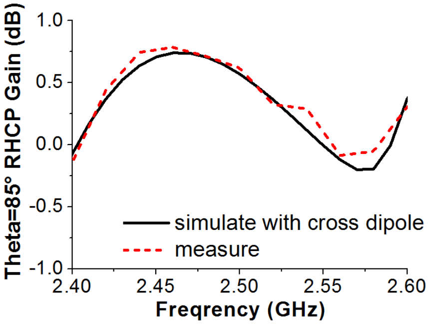

**Figure 13.** The simulated and measured results of the RHCP gain at 5° elevation angle versus frequency of the proposed antenna.

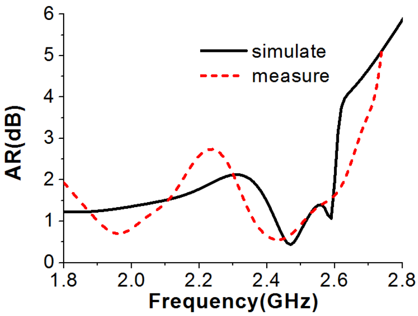

**Figure 14.** The simulated and measured results of the axial ratio at broadside versus frequency of the proposed antenna.

**Table 5.** The performance of the proposed antenna and the conventional QHA without cross dipoles.

| | Simulated conventional QHA | Simulated with cross dipole | Measured with cross dipole |
|---|---|---|---|
| 10 dB Impedance bandwidth | $> 24\%$ | | |
| 3 dB Axial ratio bandwidth | $> 32\%$ | | |
| Axial ratio (dB) | 1.8 | 0.7 | 0.9 |
| $\theta = 85^\circ$ RHCP gain (dB) | $-0.74$ | 0.65 | 0.62 |
| 3 dB Beamwidth (°) | 168 | 225 | 226 |

## 5. CONCLUSION

A simple and novel method to increase the RHCP gain at low elevation angle and widen the beamwidth of QHA has been presented in this paper. The radiation pattern, axial ratio and return loss of the proposed antenna have been analyzed and compared with that of the conventional QHA. Parametric study has been made to show how to optimize the antenna geometry to control the radiation pattern and at the same time maintain good performance in term of return loss and axial ratio.

A prototype of the QHA with cross dipoles working at 2.492 GHz for CNSS application has been realized. The RHCP gain at 5° elevation angle increases to about 0.6 dB, and the 3 dB beamwidth is more than 220°. Over the upper hemisphere, the RHCP gain is basically greater than −0.6 dB, having good cardioid shaped pattern coverage. The 10 dB impedance bandwidth is more than 24% and the 3 dB axial ratio bandwidth is more than 32%.

## ACKNOWLEDGMENT

This work was supported by the National Natural Science Foundation of China (61171029 and 61101016) and Guangzhou Science and Technology Project (12C42081659).

## REFERENCES

1. Evans, J. V., "Satellite systems for personal communications," *IEEE Trans. Antennas Propag. Mag.*, Vol. 39, 7–20, 1997.
2. Kilgus, C., "Multielement fractional turn helice," *IEEE Trans. Antennas Propag.*, Vol. 16, 499–500, 1968.
3. Kilgus, C., "Resonant quadrafilar helix design," *The Microwave J.*, Vol. 13, 49–54, 1970.
4. Adams, A., R. Greenough, R. Wallenberg, A. Mendelovicz, and C. Lumjiak, "The quadrifilar helix antenna," *IEEE Trans. Antennas Propag.*, Vol. 22, 173–178, 1974.
5. Liao, W. and Q. X. Chu, "Dual-band circularly polarized microstrip antenna with small frequency ratio," *Progress In Electromagnetics Research Letters*, Vol. 15, 145–152, 2010.
6. Li, X. H., X. S. Ren, Y. Z. Yin, L. Chen, and Z. D. Wang, "A wideband twin-diamond-shaped circularly polarized patch antenna with gap-coupled feed," *Progress In Electromagnetics Research*, Vol. 139, 15–24, 2013.
7. Deng, J. Y., Y. Z. Yin, Y. H. Huang, J. Ma, and Q. Z. Liu, "Compact circularly polarized microstrip antenna with wide beamwidth for compass satellite service," *Progress In Electromagnetics Research Letters*, Vol. 11, 113–118, 2009.
8. Yang, S. S., K. F. Lee, A. A. Kishk, and K. M. Luk, "Design and study of wideband single feed circularly polarized microstrip

antennas," *Progress In Electromagnetics Research*, Vol. 80, 45–61, 2008.

9. Deng, J. Y., L. X. Guo, T. Q. Fan, Z. S. Wu, Y. J. Hu, and J. H. Yang, "Wideband circularly polarized suspended patch antenna with indented edge and gap-coupled feed," *Progress In Electromagnetics Research*, Vol. 135, 151–159, 2013.
10. Hussein, Z. A., "Ground plane effects on quadrifilar helix antenna phase center and radiation characteristics for GPS applications," *IEEE Antennas Propag. Symp.*, Vol. 3, 1594–1597, 1991.
11. Schrott, A., M. Itaab, and H. Foster, "The antenna system of a distress buoy for use in a maritime satellite communication system (MARSAT)," *IEEE Trans. Antennas Propag.*, Vol. 24, 102–105, 1976.
12. Kazama, Y., "A quadrifilar helical antenna with parasitic loop," *IEEE Antennas Propag. Symp.*, Vol. 2, 1016–1019, 1994.
13. Kawakami, H. and G. Sato, "A quardriflar fraction-turn cone type helix antennas with reflector and cross and cross dipole," *IEE 7th International Conference on Antennas and Propagation*, Vol. 1, 34–37, 1991.
14. Chen, Z. N., W. K. Toh, and X. M. Qing, "A microstrip patch antenna with broadened beamwidth," *Microw. Opt. Technol. Lett.*, Vol. 50, No. 7, 1885–1888, 2008.
15. Latif, S. I. and L. Shafai, "Hybrid perturbation scheme for wide angle circular polarisation of stacked square-ring microstrip antenna," *Electron. Lett.*, Vol. 43, No. 20, 1065–1066, 2007.
16. Su, C. W., S. K. Huang, and C. H. Lee, "CP microstrip antenna with wide beamwidth for GPS band application," *Electron. Lett.*, Vol. 43, No. 20, 1062–1063, 2007.
17. He, H. D., "A novel wide beam circular polarization antenna — Microstrip-dielectric antenna," *Proc. Int. Conf. on Microwave and Millimeter Wave Technology*, 48–50, 2003.
18. Bao, X. L., "Dual-frequency dual circularly-polarised patch antenna with wide beamwidth," *Electron. Lett.*, Vol. 44, No. 21, 1233–1234, 2008.
19. Zhao, H. M., Y. J. Niu, and T. Liu, "A novel GPS antenna with wide beamwidth," *Proc. ICFCC*, 49–52, 2010.
20. Chu, Q. X., W. Lin, W. X. Lin, and Z. K. Pan, "Assembled dual-band broadband quadrifilar helix antennas with compact power divider networks for CNSS applications," *IEEE Trans. Antennas Propag.*, Vol. 61, No. 2, 516–523, 2013.